

Discovery of the First Topological Kondo Insulator: Samarium Hexaboride

Steven Wolgast¹, Çağlıyan Kurdak¹, Kai Sun¹, J. W. Allen¹, Dae-Jeong Kim², Zachary Fisk²

¹ *Dept. of Physics, Randall Laboratory, University of Michigan, Ann Arbor, MI 48109, USA*

² *Dept. of Physics and Astronomy, University of California at Irvine, Irvine, CA 92697, USA*

One of the most important new concepts in modern condensed matter physics is that there are new states of matter where the bulk is an unusual insulator in that it has topologically-protected metallic states on the surface. Meanwhile, in the seemingly unrelated system of strongly correlated insulators known as Kondo insulators, long-standing puzzles have remained unanswered for over thirty years. In particular, it has been found that some Kondo insulators display strange electrical transport that cannot be understood if one assumes that it is governed by the three-dimensional (3D) bulk. Here we study the transport properties of the Kondo insulator SmB_6 with a novel configuration designed to distinguish bulk-dominated conduction from surface-dominated conduction. We find that this material is a true topological insulator with a metallic surface and a fully insulating bulk, which means that its surface states can be easily studied. Thus SmB_6 is destined to be a very important material for researching the properties of topologically-protected surface states, and the discovery of the metallic surface also resolves the last remaining puzzles about the strange transport behavior of this material.

Kondo insulators^[1 - 8] (e.g. SmB_6) are a family of mixed valent or heavy fermion materials which show insulating behaviors at low temperature. Hybridization between renormalized f-electrons and conduction electrons acts to quench magnetic moments, leading to a gap above a completely filled quasi-particle band having an enormously large effective mass. For the particular case of SmB_6 , as the temperature is reduced, its resistivity increases

exponentially, as expected for an insulator with thermally activated transport. However, at lower temperatures ($T < 4$ K), the resistivity saturates and remains finite as T goes toward 0 K, in direct contrast to ordinary insulators whose resistivity diverges as T approaches 0 K. Two important puzzles remain after over thirty years. Firstly, assuming the transport is dominated by the 3D bulk, the residual resistivity cannot be successfully interpreted either as intrinsic or as an impurity band effect^[3]. Secondly, the ratio between the high-temperature and low-temperature resistivities is found to be highly non-universal and varies by orders of magnitude among different samples^[5].

The very recent theoretical prediction of topological Kondo insulators^[9–12] may shed some new light on these old puzzles. In particular, SmB_6 is predicted to be a topological Kondo insulator^[9, 12, 14], a bulk insulator with a topologically-protected metallic surface at low temperature. Despite the strong interactions, Kondo insulators share the same topological nature as weakly correlated band insulators. The topological properties in Kondo insulators are also protected by time-reversal symmetry and characterized by Z_2 topological indices (for strong and weak topological insulators). The key signatures of topological Kondo insulators, such as the existence of a metallic surface state (edge state in 2D topological insulators) characterized by Dirac cones with helical spin structures, are the same as those of other topological insulators, which have been the subject of intense theoretical investigation over the last several years^[15–24]. Topological states have been experimentally confirmed in several systems; for example, a 2D quantum spin Hall insulator state has been observed in HgTe quantum wells^[25]. Since then, 3D topological insulators have been confirmed and studied experimentally in such materials as $\text{Bi}_{1-x}\text{Sb}_x$,^[26] Bi_2Se_3 ,^[27, 28] and Bi_2Te_3 ,^[28] however, transport characterization has not been possible because the bulk of these materials is conductive. Ingenious strategies to suppress bulk conductivity, e.g. studying thin films, gating, and doping, have been employed, and sophisticated theoretical arguments are used to infer the success of these strategies. In strained HgTe^[20, 29], the quantum Hall effect has been reported for thin films with a thickness of 70 nm, where the surface contribution clearly dominates the Hall signal at mK temperatures^[30]. Quantum oscillations coming from surface states have also been observed in 3D bulk samples, e.g., $\text{Bi}_2\text{Te}_2\text{Se}$ and doped $\text{Bi}_2\text{Te}_2\text{Se}$, which

have a large bulk resistivity but are not totally insulating. It is estimated that the surface may contribute no more than 70% of the total conductance in these samples^[31, 32]. In general, identifying a material with a topologically protected surface and a fully insulating bulk would greatly simplify the study of the surface states for many important bulk-sensitive techniques.

Although SmB_6 has recently been predicted to be a topological Kondo insulator, few relevant experiments have been done. In-gap states have been reported from angle-resolved photoemission spectroscopy (ARPES)^[33], but because of the very narrow band gap and the large effective mass, the resolution is not good enough to determine whether the in-gap bands have a Dirac cone character or even whether they cross the Fermi energy.

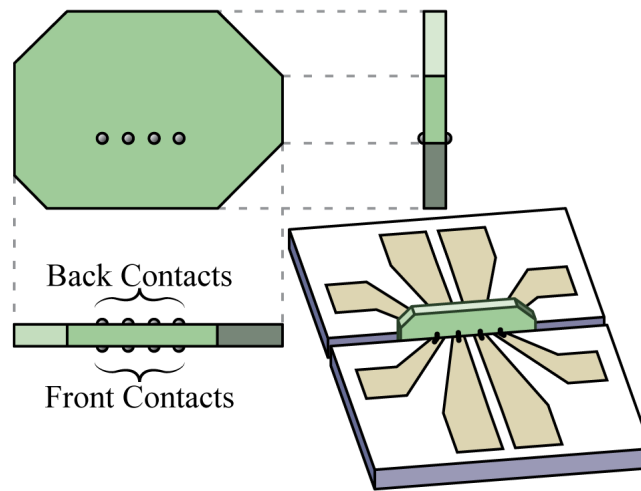


Figure 1 – Measurement geometry to distinguish bulk from surface electrical conduction – A schematic diagram of a piece of SmB_6 with 8 coplanar contacts, four on each side, is sandwiched between two silicon wafer pieces with gold contact pads.

To solve the mystery of the residual resistivity and to test the prediction of the presence of topologically-protected conducting surface states in this material, we performed transport experiments in a new type of sample geometry shown in Fig. 1. We use a thin sample of SmB_6 with eight co-planar electrical contacts, four on each side. The presence of contacts on both sides of the sample will allow us to determine whether the conduction is dominated by bulk or surface. If the material is an isotropic bulk conductor, the four-terminal resistance of the sample would be proportional to the bulk resistivity of the material with a proportionality constant that depends only on the geometry of the sample and the bulk. On

the other hand, if there is a crossover from the surface, the relative contributions from the bulk and surface resistivities can be suppressed or exaggerated depending on the position of the current and voltage leads.

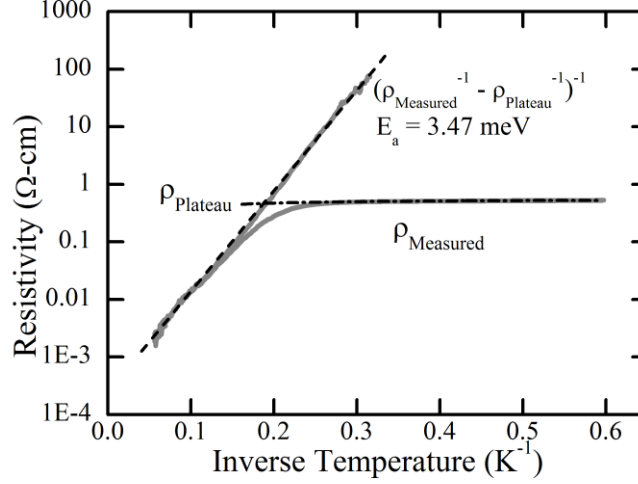


Figure 2 – Arrhenius Plot of lateral measurement data – A log plot of resistivity $\rho_{Measured}$ (solid grey line) vs inverse temperature. A linear model of the plateau resistivity $\rho_{Plateau}$ (dash-dot line) is removed from $\rho_{Measured}$ to extrapolate the bulk resistivity to 3 K. A linear fit (dashed line) yields an activation energy of 3.47 meV.

When we perform conventional four-terminal resistance measurements, just using the contacts on the front surface of the sample, we obtain data shown in Fig. 2, which is consistent with previous measurements of SmB_6 ^[3, 5], featuring a Kondo-insulator-like increase in resistivity with decreasing temperature, but with a weakly temperature-dependent plateau at low temperatures. We can model the measured conductivity as having two independent contributions: $\sigma_{Measured} = \sigma_{Insulator} + \sigma_{Plateau}$. We then extract $\sigma_{Insulator}$ down to 3 K. A linear fit of the Arrhenius plot gives us an activation energy of 3.47 meV, which is consistent with previously published measurements of SmB_6 ^[3, 5].

The plateau has never really been understood in the context of Kondo-insulator transport properties. However, with the possibility of a robust surface state, the plateau can be understood as a surface conductivity that buries the bulk conductivity at low temperatures. It is important, therefore, to determine whether the conduction at low temperatures is bulk-

dominated or surface dominated. The conventional lateral measurement R_{Lat} using contacts from one side cannot distinguish between these scenarios. However, we can explore other measurement configurations using contacts from both sides; specifically, we can make a vertical measurement R_{Vert} by passing current from one front-side contact to the back-side contact directly opposite, and measuring the voltage using a different set of opposing front-side and back-side contacts. We can also make a hybrid measurement R_{Hyb} by passing current through two front-side contacts as in the lateral measurement, but measuring the voltage on two back-side contacts. These configurations are illustrated in Fig. 3.

If the plateau is a bulk transport phenomenon, the resistance will be proportional to the resistivity for all three measurement configurations, each with a different proportionality constant. In other words, the temperature dependences of R_{Lat} , R_{Vert} , and R_{Hyb} normalized to their respective room temperature values are expected to be identical. However, if the plateau is due to surface conduction, these three four-terminal resistances behave dramatically differently as a function of temperature. We performed finite element analysis simulations of the electric potential in these two configurations on a rectangular slab with dimensions similar to our real sample and a resolution of 10 μm in each direction. Cross-sections of the slab at the contact positions are instructive for understanding our experiment design, and are shown in Fig. 3.

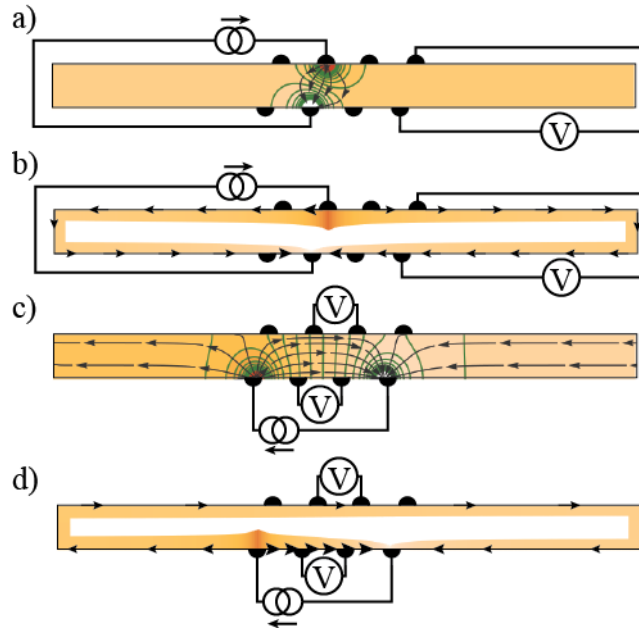


Figure 3 – Current flow and equipotential diagrams – A cross-section of the sample along the electrical contacts. Arrows indicate current direction, green lines indicate equipotentials. **a**, Current passes vertically through the bulk, far away from the voltage contacts. **b**, The bulk in **a** becomes insulating, forcing the current to flow around the edge. The surface potential is indicated by the thickness of the orange region. **c**, Current passes laterally through the bulk, and the front-side and back-side voltages are measured at similar equipotentials. **d**, The bulk in **c** becomes insulating, isolating the back-side contacts from the majority current flow.

In the vertical configuration at high temperature, nearly all the current will flow vertically directly through the sample if the bulk is conductive, as shown in Fig. 3a. Because the voltage contacts are located far away from the current, there is virtually no current near the voltage contacts, and R_{Vert} is unmeasurably small. For this reason, such a configuration is never used to measure an ordinary sample. Even though the resistivity increases significantly at low temperatures, the current will continue to flow in this configuration as long as the bulk is conductive. However, if the material becomes a surface-conductor at low temperatures, the entire current will be forced to flow around the long dimensions of the sample (Fig. 3b). In this case, the voltage contacts are very close to the current contacts, compared to the total current path around the edges; thus, R_{Vert} will become very large. Meanwhile, in the lateral configuration shown in Fig. 3c, R_{Hyb} should be nearly identical to R_{Lat} at high temperatures

when the bulk is conducting. This is because the current is nearly uniform between the front-side and back-side contacts. Again, if the bulk remains conducting at low temperatures where the resistivity becomes large, the current will still follow the same path. However, if the material becomes a surface-conductor (Fig. 3d), the back-side contacts become electrically remote from all the front-side contacts. Most of the current will flow only along the front side, and very little current will take the long path around the back side; thus R_{Hyb} will be much smaller than R_{Lat} .

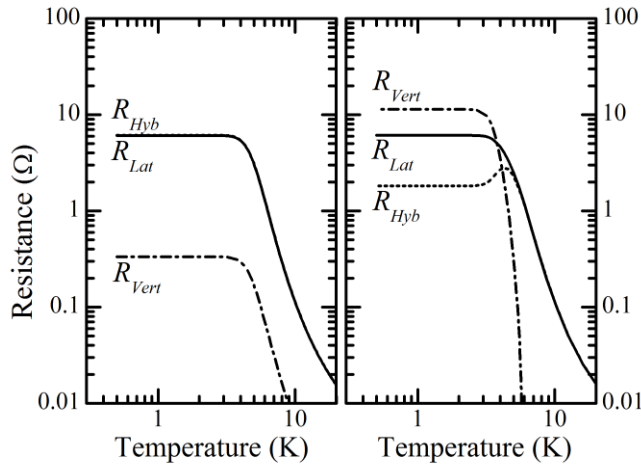


Figure 4 – Finite element analysis simulations of the experiment – Simulated log-log plots of the four-terminal resistances as a function of temperature. **Left**, the case where the saturation conductivity is a bulk phenomenon. **Right**, the case where the saturation conductivity is a surface conductivity.

The finite element analysis was performed as a function of temperature for both the bulk-only scenario and the bulk-surface crossover scenario. We assumed a system with a thermally-activated conductivity $\sigma \sim \exp(-\Delta/k_B T)$ (where Δ is the bandgap) in parallel with a constant conductivity, providing a resistivity that is qualitatively similar to previously-published measurements of SmB_6 ^[3, 5]. In the bulk-only scenario, we assume that these competing conductivities are both bulk phenomena. Figure 4a is a plot of R_{Lat} , R_{Hyb} , and R_{Vert} as a function of temperature. Because the current flow pattern does not change in this scenario, the measurements scale uniformly, each proportional to the resistivity, but with

different proportionality constants. In the bulk-surface crossover scenario, we associate the thermally-activated term with the bulk, and the constant conductivity term with the surface (Fig. 4b). Here, the measurements scale uniformly well above and below a crossover temperature, but near the crossover temperature, where $\sigma_{surface} \approx \sigma_{bulk} \times t$ (t is the thickness of the sample), the measurements do not scale with each other at all, and the proportionality relation is broken. We notice that R_{Lat} is qualitatively very similar in both configurations, making it difficult to distinguish between bulk-dominated and surface-dominated conduction from this measurement alone. We also note that in the surface-conductor case, R_{Hyb} exhibits a clear peak near the crossover temperature before settling to a smaller low-temperature value, as predicted. Finally, the change in R_{Vert} near the crossover temperature is dramatically faster than the changing resistivity.

To measure the real sample, we performed standard low-frequency lock-in measurements in the configurations described above. R_{Lat} , R_{Hyb} , and R_{Vert} are plotted in Fig. 5. The measurements behave remarkably like the crossover case of the simulations, with a distinct peak in R_{Hyb} at 3.8 K, demonstrating conclusively that SmB₆ becomes a surface-conductor below this temperature. We note in particular that R_{Lat} and R_{Hyb} scale with each other on each side of the crossover regime, suggesting the current path remains fixed. Their divergence near the crossover temperature, which corresponds to a changing current path, is effectively illustrated in the linear inset of Fig. 5. We also note that R_{Vert} increases dramatically as the temperature drops below the crossover, even more than predicted in the simulation. We attribute this discrepancy to geometrical differences between the simulated slab surface and the real sample surface. Finally, we note that below the crossover temperature, all three measurements have a weak but uniform temperature dependence.

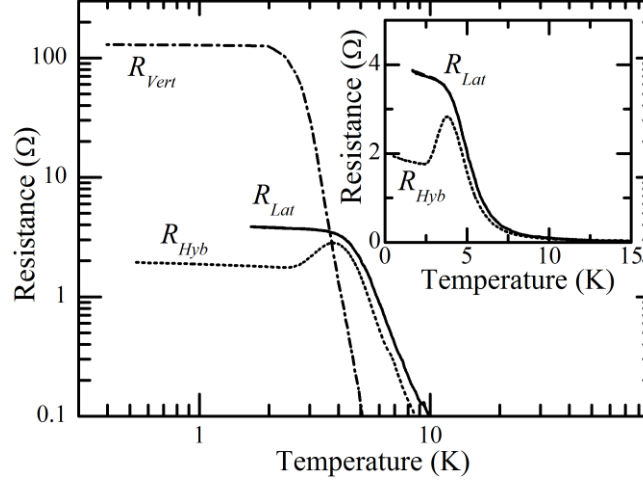


Figure 5 – Experimentally-obtained resistances as a function of temperature – A log-log plot of R_{Lat} (solid), R_{Vert} (dash-dot), and R_{Hyb} (dotted) as a function of temperature. **Inset**, a linear plot of R_{Lat} and R_{Hyb} , exaggerating the divergence between them between 3 and 5 K.

Our experiments prove unambiguously that as temperature is reduced, the system turns from a 3D bulk conductor into a 2D surface conductor with an insulating bulk. Although these measurements do not directly probe the topological nature of material, which requires spin-resolved techniques, it is worthwhile to point out that in all existing literature on SmB_6 , the residual resistivity always exists, regardless of the quality of the sample and the surface. The robustness of the surface transport strongly suggests that the surface state in SmB_6 should have some topological nature. Among all the available theories, only the topological-Kondo-insulator theory^[9] predicts the phenomena we observed. In principle, in-gap surface states can also exist in topologically trivial insulators. However, in contrast to topological surface states, the surface state in a trivial insulator is not topologically protected. These “accidental surface states” are much more vulnerable to disorder on the surface than topological surface states. First, the existence of accidental surface states relies on the quality of the surface, which varies from sample to sample. Second, even if a particular surface supports some accidental surface states at the chemical potential, these surface states are typically localized by surface disorder and thus cannot contribute to transport due to Anderson localization^[34]. However, the existence of topological surface states is guaranteed

by the nontrivial topology of the bulk, regardless of the surface's condition (as long as the time-reversal symmetry is preserved), and the disorder effects are strongly suppressed due to their helical spin structure, which suppresses backward scatterings.

This experiment also resolves the long-standing puzzles surrounding SmB_6 at low temperature. These puzzles are caused by assuming SmB_6 to be a 3D conductor. In particular, in previous studies^[3, 5], the low-temperature resistivity is computed as a 3D resistivity which, for a thin sample, is calculated as a ratio of resistance and sample thickness. This analysis is inappropriate for a 2D surface conductor, which has no sample thickness. This is one of the reasons why the ratio between the low-temperature and high-temperature resistivities varies by orders of magnitude among different samples. In addition, because low-temperature and high-temperature transport are governed by the quality of the surface and the bulk respectively, the ratio between them is expected to be non-universal, depending on the disorder in the bulk and that of the surface.

We also performed Hall effect measurements on a van der Pauw-like^[35] sample. We were able to extract the carrier concentration above the crossover temperature. However, below the crossover temperature, the Hall slope disappears, and it is no longer possible to extract the carrier density from this measurement. Nevertheless, the surface conductivity is remarkably high, which implies high mobilities. Even if we assume a carrier density as high as $5 \times 10^{14} \text{ cm}^{-2}$ (approximately 1 electron per lattice site), we get a carrier mobility of at least $1,000 \text{ cm}^2/(\text{V s})$. This high value emphasizes the robustness of the surface state and suggests that the carriers are protected from scattering mechanisms that do not flip spin. Please refer to the supplementary content for more information on this measurement.

We have conclusively demonstrated that SmB_6 exhibits a crossover near 3.8 K from bulk-dominated conduction to surface-dominated conduction; i.e., the bulk becomes insulating at temperatures below 3.8 K. In light of the robust nature of the residual resistivity

in previously published SmB₆ studies, we claim that SmB₆ is a true topological insulator that exhibits insulating bulk behavior. We note that the topological insulator surface states of SmB₆ will be easy to study. In fact, SmB₆ can be studied by any relevant technique on bulk samples with no special effort to suppress bulk conductivity beyond cooling below a readily achievable 3.8 K. Furthermore, this material is the first strongly-correlated 3D topological state of matter, which opens new opportunities to study the interplay between strong-correlation effects and topology in the search for new quantum phases, new quantum phase transitions, and new principles of physics. This result also resolves the long-standing mystery behind the low-temperature residual conductivity in the SmB₆ Kondo insulator system. We demonstrate that the Hall conductivity in the low-temperature regime is not governed by the charge Hall effect in the usual way, resolving the mystery of unphysical transport parameters in this regime. Understanding the basic transport properties of this system (e.g., carrier density, mobility) will require a great effort over a very broad range of experiments, but will allow many existing theories to be tested (e.g., Majorana fermions in a proximity-induced superconducting 3D topological insulator state^[36]), and perhaps will probe other fundamental physics.

We have also developed an effective technique for distinguishing between bulk-dominated conduction and surface-dominated conduction. Such a technique will be important for determining the bulk and surface behaviors of future 3D topological insulators. In addition to SmB₆, there are good reasons to believe that some other Kondo insulators may also be topologically nontrivial. For example, the gold phase of Samarium Sulphide (SmS) (under pressure) shows strong similarities to SmB₆^[2]. This material also satisfies the parity criterion of topological Kondo insulators^[9]. Therefore, we speculate that under pressure, SmS turns into a topological Kondo insulator.

METHODS

For our experiment, we selected a SmB_6 crystal measuring 2×1.5 mm and polished it to a thickness of $160 \mu\text{m}$, finishing with P2400 grit paper. The sample was placed into nitric and hydrochloric acids to remove aluminum flux remaining on the surface from crystal growth. For contacts, we used two $500\text{-}\mu\text{m}$ silicon wafer pieces with a 300-nm silicon oxide insulating later and lithographically patterned gold contact leads with $250\text{-}\mu\text{m}$ spacing. The pieces were cleaved across the leads, providing a flat edge on each piece to which the gold leads extended. As shown in Fig. 6, the SmB_6 sample was sandwiched between the cleaved edge of the wafer pieces and glued into place with Varian Torr Seal. The gap between the sample and the cleaved surface edge varied from < 5 to $30 \mu\text{m}$. We observed epoxy wetting in portions of the gaps.

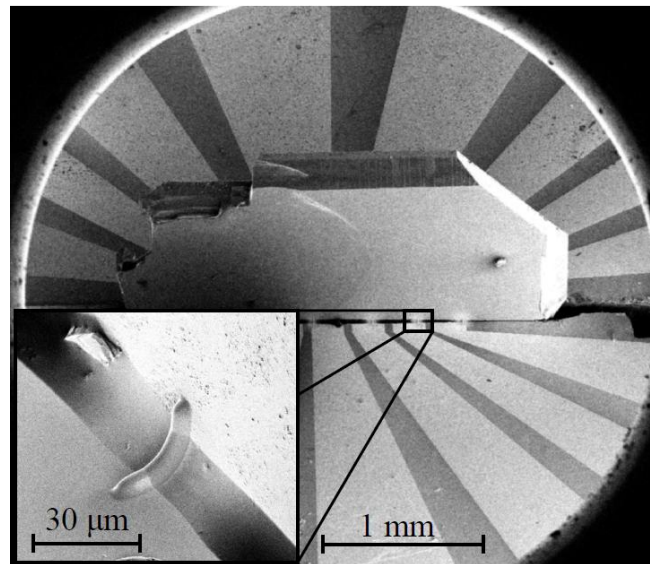


Figure 6 – SEM image of SmB_6 sample – A scanning electron microscope image of a single-crystal of SmB_6 , sandwiched between two silicon wafer pieces with lithographically-defined contact pads. **Inset**, a close-up of one of the platinum contacts connecting the SmB_6 to a gold contact pad.

We deposited platinum contact wires connecting the SmB_6 to the gold leads using ion beam-induced deposition (Fig. 6 inset). The ion beam was incident on the sample at 52° . The wires were $3 \mu\text{m}$ wide and $1\text{--}3 \mu\text{m}$ thick, with a length sufficient to span the gap between the SmB_6 and the gold lead, varying from 20 to $50 \mu\text{m}$. The epoxy wetting served as an insulating “bridge” for the platinum between the SmB_6 and some of the gold leads. It was possible to

deposit a wire in a few places without the epoxy bridge, provided the gap was smaller than 10 μm ; a few of these were reliable and Ohmic even at cryogenic temperatures.

REFERENCES

- [1] A. Menth, E. Buehler, and T. H. Geballe, "Magnetic and Semiconducting Properties of SmB_6 ," *Phys. Rev. Lett.* **22**, 295 (1969)
- [2] R. M. Martin and J. W. Allen, "Theory of mixed valence: Metals or small gap insulators," *J. Appl. Phys.* **50**, 7561 (1979)
- [3] J. W. Allen, B. Batlogg, and P. Wachter, "Large low-temperature Hall effect and resistivity in mixed-valent SmB_6 ," *Phys. Rev. B* **20**, 4807–4813 (1979)
- [4] G. Aeppli and Z. Fisk, "Kondo Insulators," *Comm. Condens. Matter Phys.* **16**, 155 (1992)
- [5] J. C. Cooley, M. C. Aronson, Z. Fisk, and P. C. Canfield, "SmB₆: Kondo Insulator or Exotic Metal?" *Phys. Rev. Lett.* **74**, 1629-1632 (1995)
- [6] H. Tsunetsugu, M. Sigrist and K. Ueda, "The ground-state phase diagram of the one-dimensional Kondo lattice model," *Rev. Mod. Phys.* **69**, 809 (1997)
- [7] P. Riseborough, "Heavy fermion semiconductors," *Adv. Phys.* **49**, 257 (2000)
- [8] P. Coleman, "Heavy Fermions: Electrons at the Edge of Magnetism", *Handbook of Magnetism and Advanced Magnetic Materials*, Vol **1**, 95-148 (Wiley, 2007)
- [9] M. Dzero, K. Sun, V. Galitski, and P. Coleman, "Topological Kondo Insulators," *Phys. Rev. Lett.* **104**, 106408 (2010)
- [10] Alexey A. Soluyanov and David Vanderbilt, "Wannier representation of Z_2 topological insulators", *Phys. Rev. B* **83**, 035108 (2011)
- [11] Rui Yu, Xiao-Liang Qi, Andrei Bernevig, Zhong Fang, and Xi Dai, "Equivalent expression of Z_2 topological invariant for band insulators using the non-Abelian Berry connection," *Phys. Rev. B* **84**, 075119 (2011)

- [12] M. Dzero, K. Sun, P. Coleman, and V. Galitski, "Theory of topological Kondo insulators," *Phys. Rev. B* **85**, 045130 (2012)
- [13] T. Takimoto, "SmB₆: A Promising Candidate for a Topological Insulator," *Journal of the Physical Society of Japan* **80**, 123710 (2011)
- [14] D. J. Kim, T. Grant, and Z. Fisk, "Limit Cycle and Anomalous Capacitance in the Kondo Insulator SmB₆," *Phys. Rev. Lett.* **109**, 096601 (2012)
- [15] C. L. Kane and E. J. Mele, "Quantum Spin Hall Effect in Graphene," *Phys. Rev. Lett.* **95**, 226801 (2005)
- [16] C. L. Kane and E. J. Mele, "Z₂ Topological Order and the Quantum Spin Hall Effect," *Phys. Rev. Lett.* **95**, 146802 (2005)
- [17] B. A. Bernevig, T. L. Hughes, and S.-C. Zhang, "Quantum Spin Hall Effect and Topological Phase Transition in HgTe Quantum Wells," *Science* **314**, 1757-1761 (2006)
- [18] L. Fu, C. L. Kane, and E. J. Mele, "Topological Insulators in Three Dimensions," *Phys. Rev. Lett.* **98**, 106803 (2007)
- [19] J. E. Moore and L. Balents, "Topological invariants of time-reversal-invariant band structures," *Phys. Rev. B* **75**, 121306 (2007)
- [20] L. Fu and C. L. Kane, "Topological insulators with inversion symmetry," *Phys. Rev. B* **76**, 045302 (2007)
- [21] R. Roy, "Topological phases and the quantum spin Hall effect in three dimensions," *Phys. Rev. B* **79**, 195322 (2009)
- [22] M. Z. Hasan and C. L. Kane, "Colloquium: Topological insulators," *Reviews of Modern Physics* **82**, 3045-3067 (2010)
- [23] J. E. Moore, "The birth of topological insulators," *Nature* **464**, 194-198 (2010)
- [24] X.-L. Qi and S.-C. Zhang, "Topological insulators and superconductors," *Reviews of Modern Physics* **83**, 1057-1110 (2011)

- [25] M. König, et.al., “Quantum Spin Hall Insulator State in HgTe Quantum Wells.” *Science* **318**, 766-770 (2007)
- [26] D. Hsieh, D. Qian, L. Wray, Y. Xia, Y. S. Hor, R. J. Cava, and M. Z. Hasan, "A topological Dirac insulator in a quantum spin Hall phase," *Nature* **452**, 970-974 (2008)
- [27] Y. Xia, D. Qian, D. Hsieh, L. Wray, A. Pal, H. Lin, A. Bansil, D. Grauer, Y. S. Hor, R. J. Cava, and M. Z. Hasan, "Observation of a large-gap topological-insulator class with a single Dirac cone on the surface," *Nat Phys.* **5**, 398-402 (2009)
- [28] H. Zhang, C.-X. Liu, X.-L. Qi, X. Dai, Z. Fang, and S.-C. Zhang, "Topological insulators in Bi₂Se₃, Bi₂Te₃ and Sb₂Te₃ with a single Dirac cone on the surface," *Nat Phys.* **5**, 438-442 (2009)
- [29] X. Dai, T. L. Hughes, X.-L. Qi, Z. Fang, and S.-C. Zhang, “Helical edge and surface states in HgTe quantum wells and bulk insulators.” *Phys. Rev. B* **77**, 125319 (2008)
- [30] C. Brüne, et.al., “Quantum Hall Effect from the Topological Surface States of Strained Bulk HgTe.” *Phys. Rev. Lett.* **106**, 126803 (2011)
- [31] A. A. Taskin, Z. Ren, S. Sasaki, K. Segawa, and Y. Ando, “Observation of Dirac Holes and Electrons in a Topological Insulator.” *Phys. Rev. Lett.* **107**, 016801 (2011)
- [32] J. Xiong, et.al., “Quantum oscillations in a topological insulator Bi₂Te₂Se with large bulk resistivity (6 Ω cm).” *Physica E* **44**, 917-920 (2012)
- [33] H. Miyazaki, T. Hajiri, T. Ito, S. Kunii, and S. I. Kimura, “Momentum-dependent hybridization gap and dispersive in-gap state of the Kondo semiconductor SmB₆,” *Phys. Rev. B* **86**, 075105 (2012)
- [34] P.W. Anderson, “Absence of Diffusion in Certain Random Lattices,” *Phys. Rev.* **109**, 1492 (1958)
- [35] L. J. van der Pauw, “A Method of Measuring the Resistivity and Hall Coefficient on Lamellae of Arbitrary Shape,” *Philips Tech. Rev.* **20**, 220-224 (1958)

[36] L. Fu and C. L. Kane, “Superconducting Proximity Effect and Majorana Fermions at the Surface of a Topological Insulator,” *Phys. Rev. Lett.* **100**, 096407 (2008)

Acknowledgements

This project was performed in part in the Electron Microbeam Analysis Laboratory (EMAL), which is supported by NSF grant #DMR-0320740, and in the Lurie Nanofabrication Facility (LNF), a member of the National Nanotechnology Infrastructure Network, which is supported by the National Science Foundation. The portion performed at the University of Michigan was supported by NSF grant #DMR-1006500. The portion performed at the University of California at Irvine was supported by NSF grant #DMR-0801253. The authors wish to acknowledge Richard Field III for his photography services, Yun Suk Eo for assisting with the experiment, Ilya Vugmeyster for help with polishing, Jason Cooley for sample preparation advice, Emanuel Gull for helpful discussions on numerical techniques, and Piers Coleman and Shou-Cheng Zhang for advice on improving the manuscript.

Contributions

S. Wolgast fabricated the samples and performed the measurements. C. Kurdak designed the experiment. K. Sun suggested the study of the residual resistivity in this material and performed the FEA simulations. J. Allen assembled the research team. D. J. Kim and Z. Fisk grew the SmB_6 crystals. The authors at Michigan all participated in discussion of the results and writing of the manuscript.

Competing Financial Interests

The authors declare no competing financial interests.

Correspondence

Correspondence and requests for materials should be addressed to Cagliyan Kurdak (kurdak@umich.edu).

Supplementary Information

We prepared a van der Pauw-like geometry for measurements of resistivity and Hall conduction. The sample is $3.47 \text{ mm} \times 1.32 \text{ mm} \times 170 \text{ }\mu\text{m}$, and the two large faces were polished with P4000 grit paper. The sample was mounted to a glass substrate with Varian Torr Seal, and indium contacts were placed along the edge (Fig. S1). Two leads extended along the short edges to function as current leads, while four additional leads were placed along the long edges, two on each side, for voltage contacts.

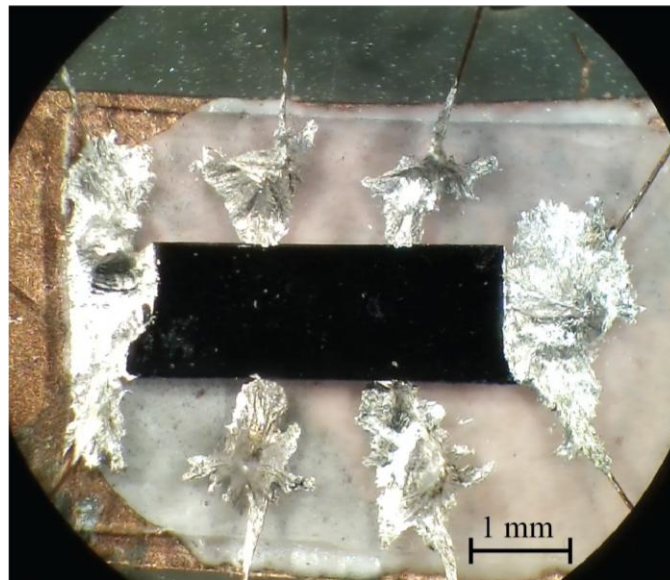


Figure S1 – Image of van der Pauw sample – Image showing the contact positions on the van der Pauw sample.

We measured the Hall conductivity using lock-in techniques at 26.6 Hz in a ^3He cryostat. We swept the magnetic field between -8 and 8 T perpendicular to the flat surfaces of the sample. For an ordinary material, this measurement provides us with the carrier density. However, for the topological surface state, this is not the case. Although the top and bottom surfaces are perpendicular to the magnetic field, there are also side surfaces parallel to the magnetic field. The top and bottom surfaces can be considered as two parallel Hall bars, but the side surfaces, which show no Hall effect, add a metallic shell to the edges of these two Hall bars and suppress the Hall voltage significantly. This is indeed what we observed. We

obtained a sheet resistance of 9.1Ω . Below the crossover temperature, the Hall measurement was anomalous, with no detectable slope and a large temperature-dependent feature near 0-field (Fig. S2). If one naively calculates the carrier density from the Hall resistivity like in an ordinary Hall bar using $n_{2D} = B/eR_H$, one gets a carrier concentration that is unphysically large. We note that analyzing low-temperature carrier concentration measurements made by prior studies as two-dimensional concentrations gives likewise unphysical results. Because the conduction in these samples is unambiguously dominated by surface currents at low temperatures, the usual calculation for n_{2D} must be invalid for such systems. Nevertheless, the surface conductivity is remarkably high, which implies high mobilities. Even if we assume a carrier density as high as $5 \times 10^{14} \text{ cm}^{-2}$ (approximately 1 electron per lattice site), we get a carrier mobility of at least $1,000 \text{ cm}^2/(\text{V s})$. This high value emphasizes the robustness of the surface state and suggests that the carriers are protected from scattering mechanisms that do not flip spin.

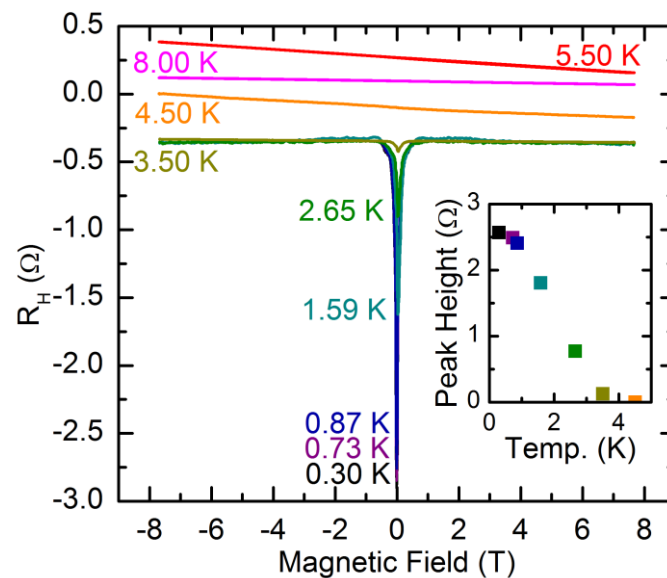


Figure S2 – Plot of Hall resistance vs magnetic field – Plots of Hall resistance at several temperatures as a function of magnetic field. At the crossover, the Hall slope disappears, and a 0-field feature appears. **Inset**, a plot of the feature peak height as a function of temperature.